

ChemComm

Porphyritic supramolecular daisy chains incorporating pillar[5]arene-viologen host-guest interactions

Maher Fathalla,^{a,c} Nathan L. Strutt,^a Srinivasan Sampath,^a Khabiboulakh Katsiev,^b
Karel J. Hartlieb,^a Osman M. Bakr,^b J. Fraser Stoddart^{*a}

^a Center for the Chemistry of Integrated Systems, Department of Chemistry, Northwestern University,
2145 Sheridan Road, Evanston, IL 60208, USA.

^b Division of Physical Sciences and Engineering, Solar and Photovoltaics Engineering Center,
King Abdullah University of Science and Technology (KAUST), Thuwal 23955-6900, Saudi Arabia.

^c Present address: Department of Chemistry Faculty of Science, Zagazig University, Zagazig, Egypt.

Supporting Information

Table of Contents

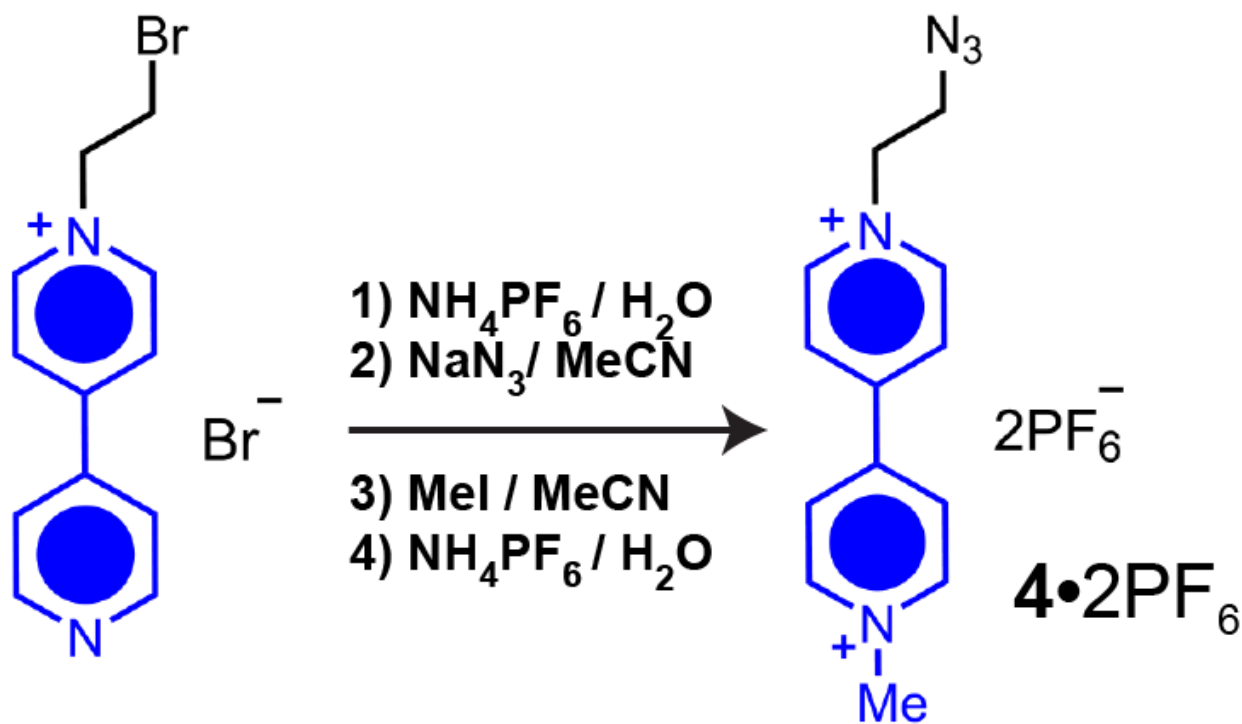
S1. General Methods	S2
S2. Synthetic Procedures	S3
S3. UV-Vis and Fluorescence Spectra	S7
S4. Molecular Modelling	S8
S5. DLS Measurements	S9
S6. TEM Images	S10
S7. SEM Images	S11
S8. References	S13

S1. General Methods

All reagents were purchased from commercial suppliers (Aldrich or Fisher) and used without further purification. Thin-layer chromatography (TLC) was performed on silica gel 60 F254 TLC plates (Merck). Column chromatography was carried out on silica gel 60F (Merck 9385; 0.040–0.063 mm). Deuterated solvents (Cambridge Isotope Laboratories) for NMR spectroscopic analyses were used as received. Solution ^1H NMR spectra were recorded on Bruker Avance-500 spectrometers at 500 MHz at ambient temperature. All chemical shifts are quoted in ppm relative to the signals corresponding to the residual non-deuterated solvents (CDCl_3 : $\delta_{\text{H}} = 7.26$ ppm, CD_3CN : $\delta_{\text{H}} = 1.94$ ppm). The following abbreviations are used to explain the multiplicities: s, singlet; d, doublet; t, triplet; b, broad peaks; m, multiplet or overlapping peaks. High-resolution mass spectra (HRMS) were measured on an Agilent 6210 Time of Flight (TOF) LC-MS, using an ESI source, coupled with Agilent 1100 HPLC stack, using direct infusion (0.6 mL min^{-1}). UV/Vis Absorbance spectra were recorded using a UV-3600 Shimadzu spectrophotometer. The fluorescence spectra were obtained on a Shimadzu RF-5301 PC spectrofluorophotometer, using a quartz cell. DLS measurements were carried out with a Zetasizer Nano ZS instrument purchased from Malvern Instruments Ltd. at 298K using a 633 nm laser. The mean hydrodynamic radius was calculated with Zetasizer software. Transmission electron microscopy (TEM) was conducted using TEM-JEOL-2100F instrument at a 200 kV accelerating electron voltage. SEM imaging was performed on a FEI Quanta 600F sFEG ESEM scanning electron microscope (SEM) at an accelerating electron voltage of 30 kV. Rheological measurements were performed using a modular compact rheometer Anton Paar MCR150 Physica instrument with 25 mm diameter parallel plate geometry. STM Measurements were carried out in an ultrahigh vacuum (UHV) chamber with a base pressure of $\sim 2 \times 10^{-10}$ Torr. The chamber was equipped with the variable temperature scanning tunneling microscope (STM) Omicron VT STM XA 50/500, SPHERA U7 hemispherical energy analyzer with 7 channel MCD detector, high intensity He I/II lamp HIS 13 ultraviolet photon source, XM 1000 monochromated X-ray source: high intensity, high energy resolution monochromated Al $K\alpha$ X-ray source with 500 mm Rowland circle diameter, minimum spot size ~ 1 mm, photon line width < 250 meV. STM images were acquired at room temperature in a constant current mode. Electrochemically etched W tip was used for all the measurements.

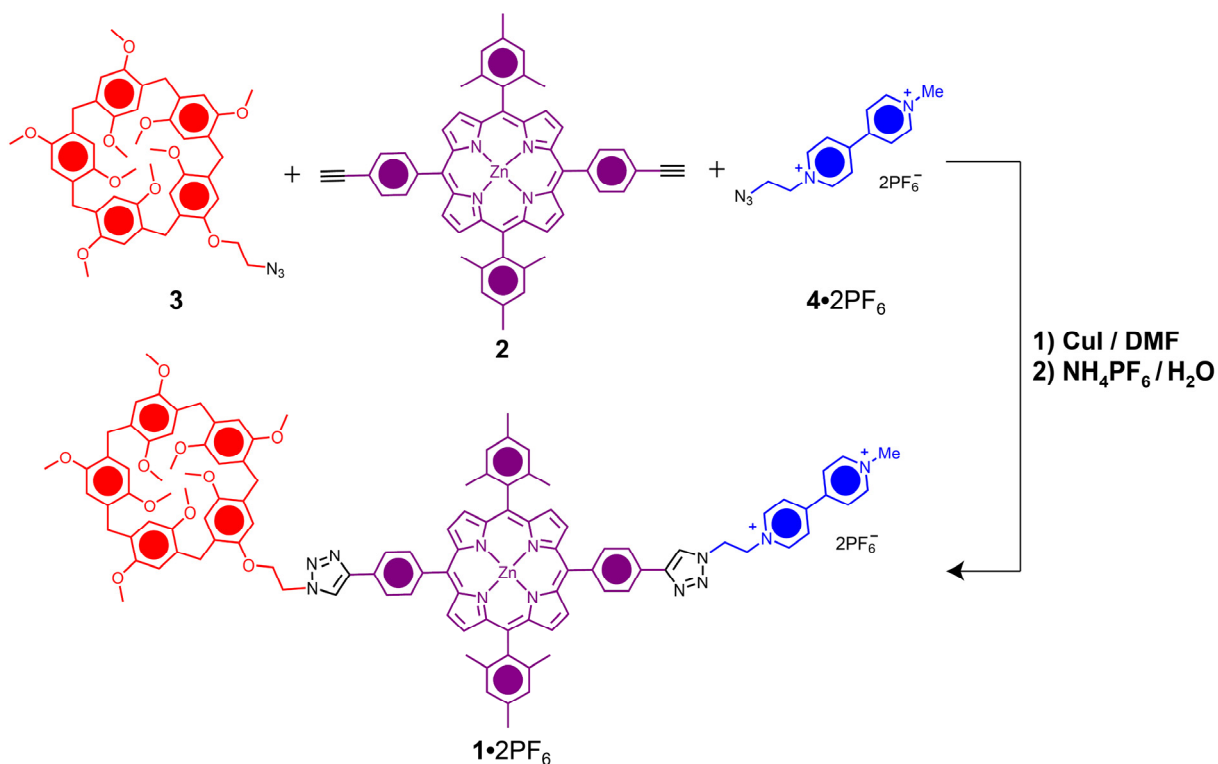
S2. Synthetic Procedures

4•2PF₆: NH₄PF₆ (2.00 g, 12.2 mmol) was added to a solution of 1-(2-bromoethyl)-4,4'-pyridylpyridinium bromide^{S1} (2.00 g, 5.81 mmol) in H₂O (100 mL). The precipitate which forms was collected, washed thoroughly with H₂O and dried in vacuo. This solid was then added to a suspension of NaN₃ (0.75 g, 11.5 mmol) in MeCN (50 mL). The reaction mixture was stirred at rt for 12 h and added to H₂O (50 mL). The MeCN was removed in vacuo and the formed precipitate was collected, washed with H₂O and dried in vacuo. This solid was then added to a solution of MeI (1.0 g, 7.0 mmol) in MeCN (50 mL) and the reaction mixture was stirred at 80°C for 12 h. Hexane (100 mL) was added to the reaction mixture and the formed precipitate was collected and washed with an excess of hexane. The residual solid was dissolved in H₂O (50 mL) and treated with an excess of NH₄PF₆ (2.00 g, 12.2 mmol). The precipitate was collected, washed thoroughly with H₂O and dried in vacuo to give **4•2PF₆** (2.0 g, 61%).

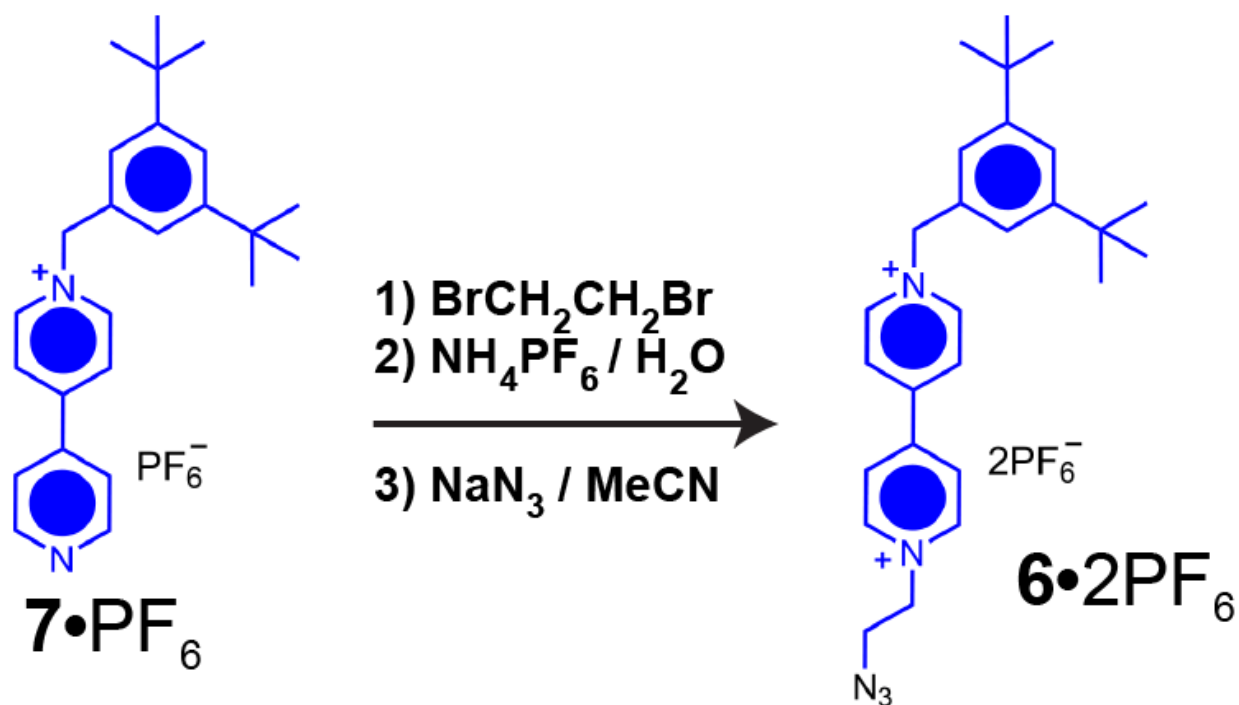


¹H NMR (500 MHz, CD₃CN, 298 K) δ = 8.90 (d, J = 7 Hz, 2H), 8.85 (d, J = 6.5 Hz, 2H), 8.41 (d, J = 7 Hz, 2H), 8.37 (d, J = 6.5 Hz, 2H), 4.73 (t, J = 5.5 Hz, 2H), 4.40 (s, 3H), 4.00 (t, J = 5.5 Hz, 2H). ¹³C NMR (125 MHz, CD₃CN, 298 K) δ = 151.5, 150.5, 147.5, 147.0, 128.1, 127.8, 61.6, 51.2, 49.6. HRMS: (m/z): calcd for [$M - \text{PF}_6$]⁺: 386.0964; found 386.0963.

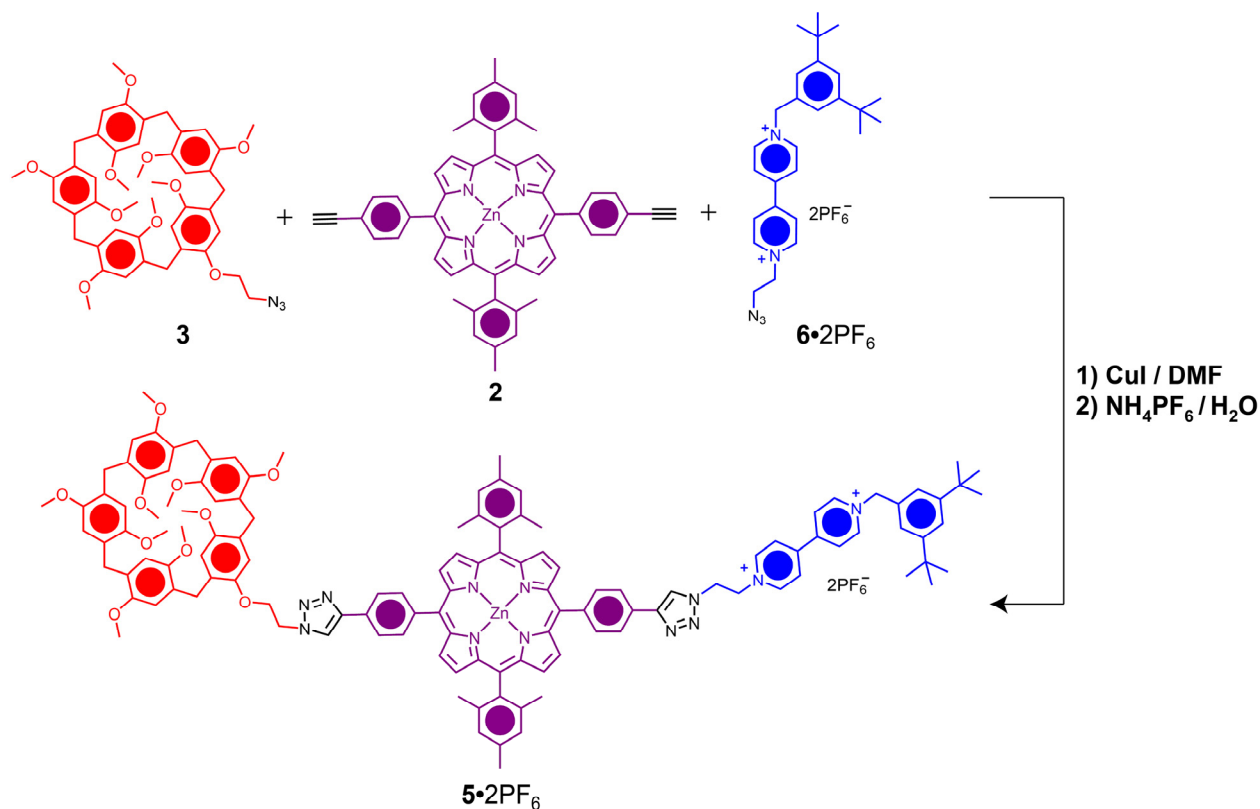
1•2PF₆: A solution of porphyrin **2** (50 mg, 0.062 mmol), **3**^{S₂} (54 mg, 0.067 mmol) and **4**•2PF₆ (36 mg, 0.067 mmol) in dry DMF (8 mL) was degassed with Ar for 1 h. CuI (15 mg) was then added and the reaction was degassed for an additional 1h before heating at 60 °C for 40 h. The solvent was removed in vacuo and the crude product was subjected to column chromatography (SiO₂, Me₂CO→3% NH₄PF₆/Me₂CO) to give **1**•2PF₆ as a purple solid (60 mg, 45 %).



¹H NMR (500 MHz, CD₃CN, 298 K) δ = 8.89 (d, 2H), 8.86 (d, 2H), 8.84 (m, 4H), 8.65 (m, 4H), 8.53 (s, 1H), 8.46 (d, 2H), 8.44 (s, 1H), 8.41 (d, 2H), 8.29 (d, 2H), 8.23 (m, 6H), 7.32 (s, 4H), 6.88 (m, 10H), 5.28 (t, 2H), 5.18 (t, 2H), 4.93 (t, 2H), 4.44 (t, 2H), 4.40 (s, 3H), 3.72 (m, 37H), 2.59 (s, 6H), 1.80 (s, 12H). ¹³C NMR (125 MHz, CD₃CN, 298 K) δ = 152.0, 151.7, 151.2, 151.13, 151.1, 151.0, 150.99, 150.9, 150.6, 150.5, 150.4, 150.2, 149.4, 148.5, 148.0, 147.4, 147.1, 144.0, 143.5, 140.1, 139.8, 138.6, 135.8, 135.6, 133.0, 132.7, 131.3, 131.28, 131.1, 130.5, 130.3, 129.4, 129.3, 129.0, 128.3, 127.9, 124.6, 124.5, 123.1, 122.6, 120.5, 120.1, 119.7, 116.3, 114.2, 114.14, 114.1, 114.0, 113.98, 113.83, 113.80, 113.7, 68.6, 61.9, 56.4, 56.3, 56.2, 56.16, 56.1, 55.9, 51.3, 50.7, 49.6, 30.8, 30.2, 30.1, 29.8, 29.6, 29.3, 21.8, 21.4. HRMS: (*m/z*): calcd for [*M* - PF₆]⁺: 1853.7362; found 1853.7266; calcd for [*M* - 2PF₆]²⁺: 927.3717; found 927.3717. UV-vis (CH₂Cl₂): 422 (ϵ 282 000 dm³ mol⁻¹ cm⁻¹), 550 (19 050), 589 (5 650).



6·2PF₆: 1,2-Dibromoethane (0.470 g, 2.50 mmol) was added to a solution of 3,5-di-*tert*-butylbenzyl-4,4'-pyridylpyridinium hexafluorophosphate^{S3} **7·PF₆** (1.00 g, 1.98 mmol) in MeCN (100 mL). The reaction mixture was stirred at 80°C for 12 h, cooled to room temperature and the solvent was removed in vacuo. The residual solid was dissolved in H₂O and treated with excess of NH₄PF₆ (1.00 g, 6.16 mmol). The precipitate which formed was collected, washed thoroughly with H₂O and dried in vacuo. This residual solid was then added to a suspension of NaN₃ (0.50 g, 7.7 mmol) in MeCN (50 mL). The reaction mixture was stirred at rt for 12 h before being added to H₂O (50 mL). The MeCN was removed in vacuo and the precipitate formed was collected, washed with H₂O and dried in vacuo to give **6·2PF₆** (0.66 g, 46%). ¹H NMR (500 MHz, CD₃CN, 298 K) δ = 9.00 (d, *J* = 5 Hz, 2H), 8.89 (d, *J* = 5 Hz, 2H), 8.38 (m, 4H), 7.59 (t, *J* = 1.5 Hz, 1H), 7.41 (d, *J* = 1.5 Hz, 2H), 5.77 (s, 2H), 4.73 (t, *J* = 5.5 Hz, 2H), 4.00 (t, *J* = 5.5 Hz, 2H), 1.33 (s, 18H). ¹³C NMR (125 MHz, CD₃CN, 298 K) δ = 153.5, 151.5, 151.1, 147.0, 146.4, 132.9, 128.5, 128.1, 125.3, 124.8, 66.4, 61.6, 51.2, 35.7, 31.4. HRMS: (*m/z*): calcd for [*M* - PF₆]⁺: 574.2529; found 574.2543.



5·2PF₆: A solution of porphyrin **2** (50 mg, 0.062 mmol), **3** (54 mg, 0.067 mmol) and **6·2PF₆** (48 mg, 0.067 mmol) in dry DMF (8 mL) was degassed with Ar for 1 h. CuI (15 mg) was then added and the reaction was degassed for additional 1 h before heating at 60 °C for 40 h. The solvent was removed in vacuo and the crude product was subjected to column chromatography (SiO₂, Me₂CO→1% NH₄PF₆/Me₂CO) to give **5·2PF₆** as a purple solid (80 mg, 55%). ¹H NMR (500 MHz, CD₃CN, 298 K) δ = 9.01 (d, 2H), 8.88 (d, 2H), 8.85 (d, 2H), 8.82 (d, 2H), 8.66 (m, 4H), 8.53 (s, 1H), 8.44 (d, 2H), 8.42 (s, 1H), 8.40 (d, 2H), 8.28 (d, 2H), 8.21 (m, 6H), 7.57 (t, 1H), 7.40 (d, 2H), 7.33 (s, 4H), 6.89 (m, 10H), 5.76 (s, 2H), 5.28 (t, 2H), 5.18 (t, 2H), 4.93 (t, 2H), 4.44 (t, 2H), 3.72 (m, 37H), 2.59 (s, 6H), 1.80 (s, 12H), 1.31 (s, 18H). ¹³C NMR (125 MHz, CD₃CN, 298 K) δ = 153.4, 151.9, 151.7, 151.0, 150.8, 150.6, 150.5, 150.4, 149.4, 148.5, 148.0, 147.1, 146.3, 144.0, 143.4, 140.1, 139.8, 138.5, 135.7, 135.6, 133.0, 132.9, 131.3, 131.0, 130.9, 130.2, 129.0, 128.5, 128.4, 128.3, 125.2, 124.7, 124.6, 124.4, 123.1, 122.6, 120.5, 120.1, 119.6, 116.2, 114.1, 113.9, 113.8, 113.5, 68.5, 66.3, 61.8, 56.4, 56.2, 56.1, 55.9, 51.2, 50.7, 49.6, 35.6, 31.4, 30.8, 30.1, 29.8, 29.6, 29.2, 25.9, 21.8, 21.4. HRMS: (*m/z*): calcd for [*M* – PF₆]⁺: 2187.8646; found 2187.8635; calcd for [*M* – 2PF₆]²⁺: 1021.4502; found 1021.4520. UV-vis (CH₂Cl₂): 422 (ε 366 500 dm³ mol⁻¹ cm⁻¹), 550 (21 550), 590 (4 650).

S3. UV-Vis and Fluorescence Spectra

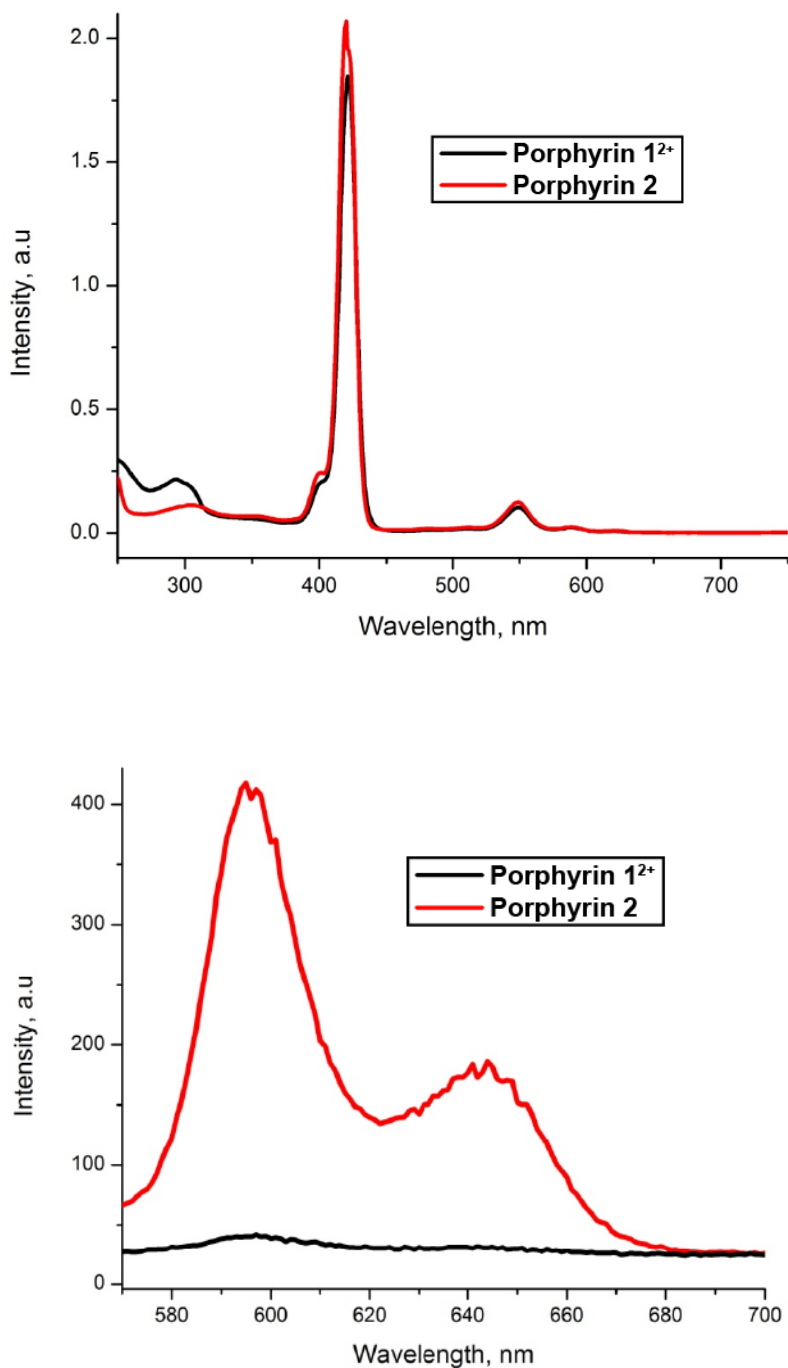


Figure S1. UV-Vis (top) and fluorescence (bottom) spectra of porphyrin 1^{2+} and **2** in CH_2Cl_2 ($5 \mu\text{m}$, $\lambda_{\text{ex}} = 555 \text{ nm}$)

S4. Molecular Modelling

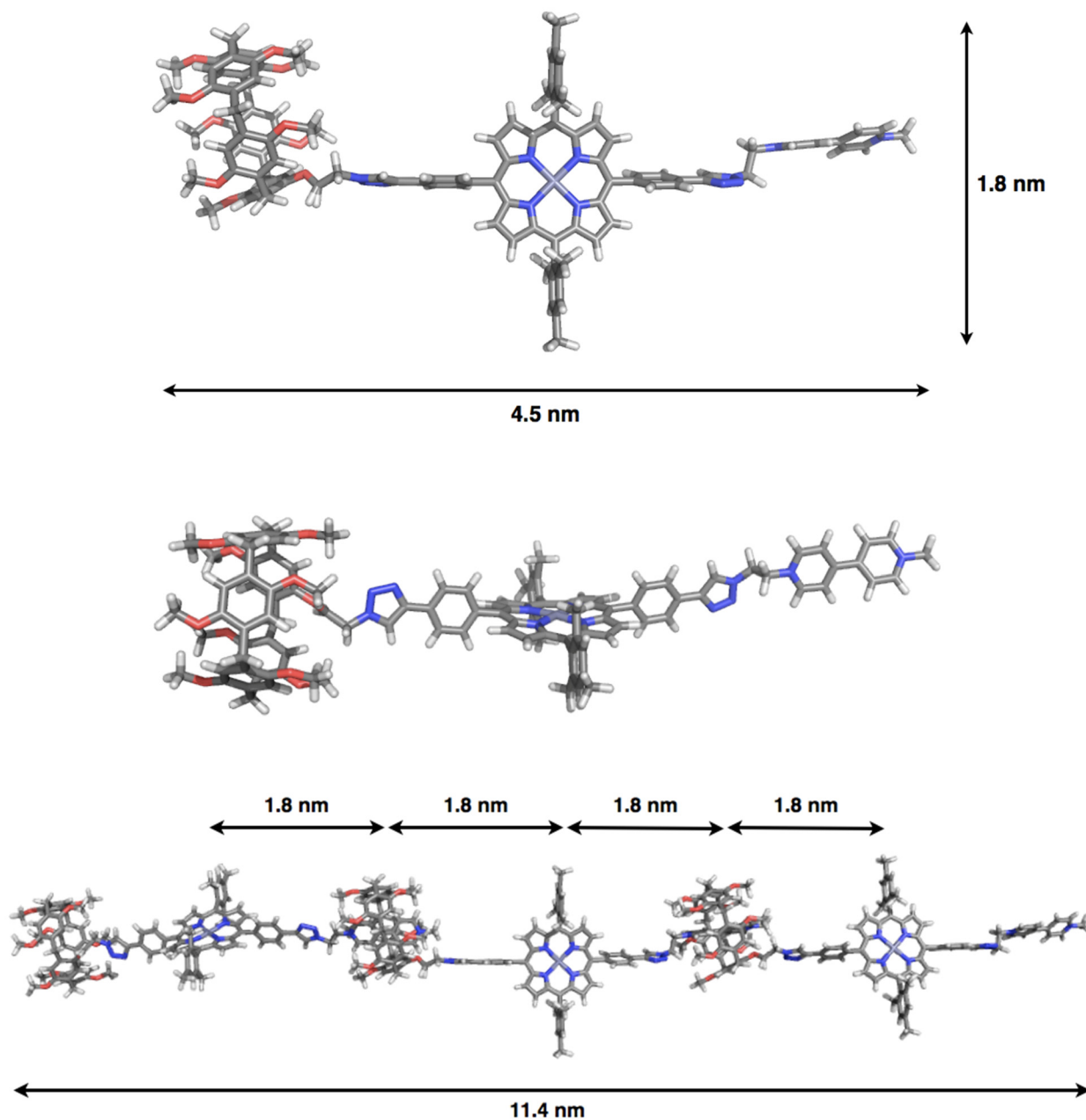


Figure S2. Molecular modeling for porphyrin $1 \cdot 2PF_6$ and daisy chains from $1 \cdot 2PF_6$. Hyperchem was used to build the structures followed by optimization using MM+. Counterions were omitted. The distance between the porphyrin macrocycle and the (1:1) P5A-viologen complex (1.8 nm) is in a good agreement with the distance (1.7 nm) between the bright spots in the STM measurements

S5. DLS Measurements

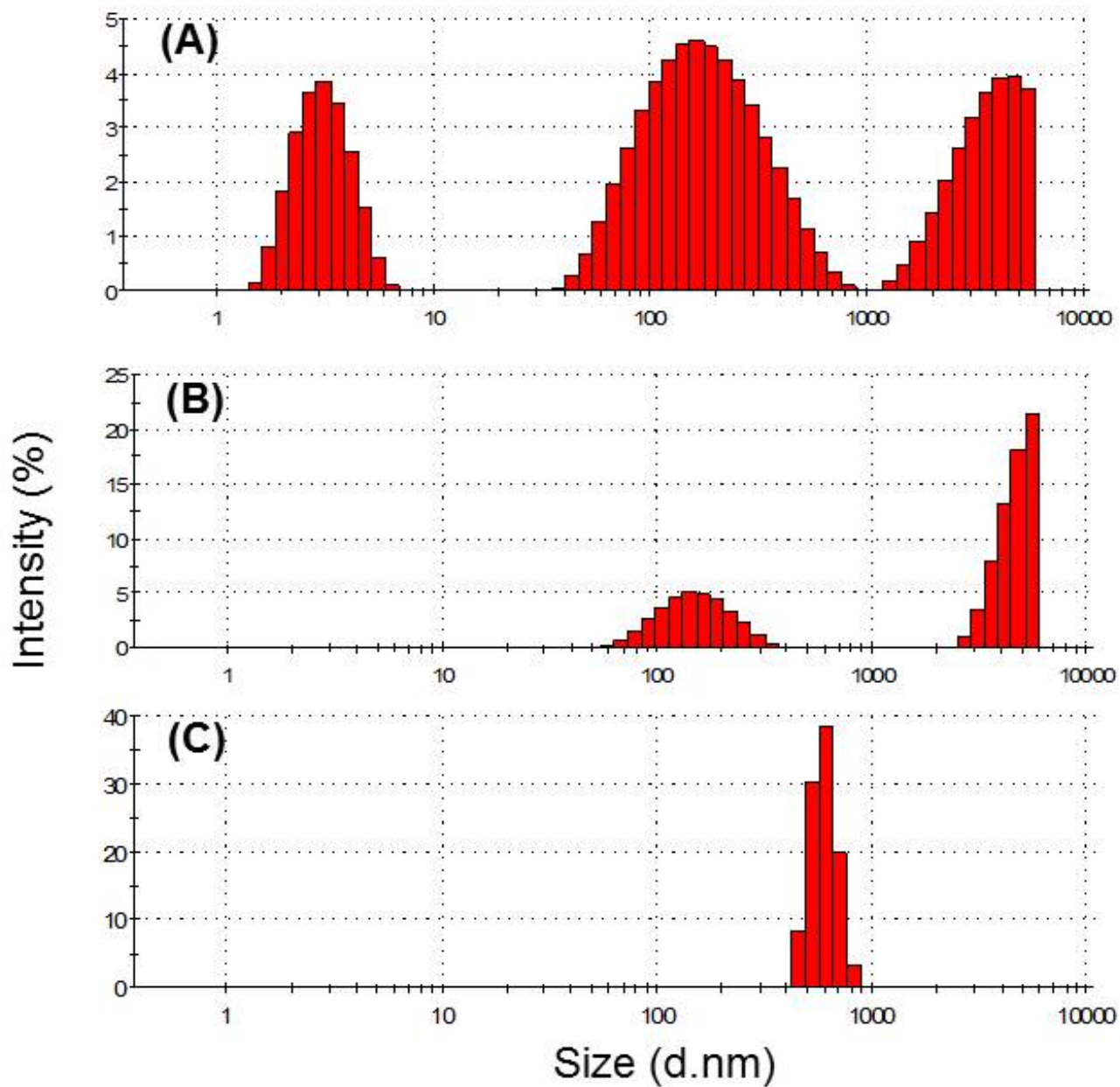


Figure S3. DLS Measurements of the resulting daisy chains from $1 \cdot 2\text{PF}_6$ in CH_2Cl_2 over a range of concentrations [(A) = 1, (B) = 5 and (C) = 10 μm]

S6. TEM Images

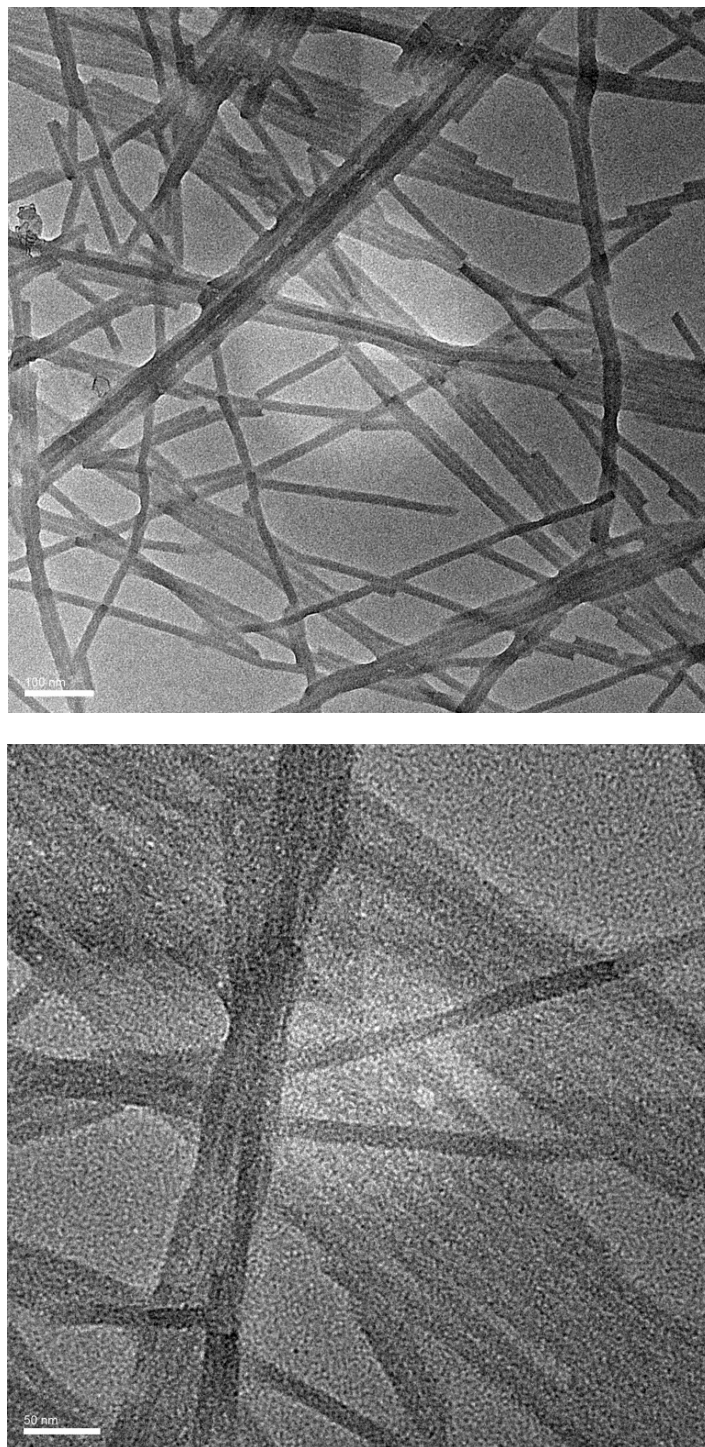


Figure S4. TEM Images of daisy chains from $1 \cdot 2PF_6$ in CH_2Cl_2 . Scale: 100 nm (top), 50 nm (bottom)

S7. SEM Images

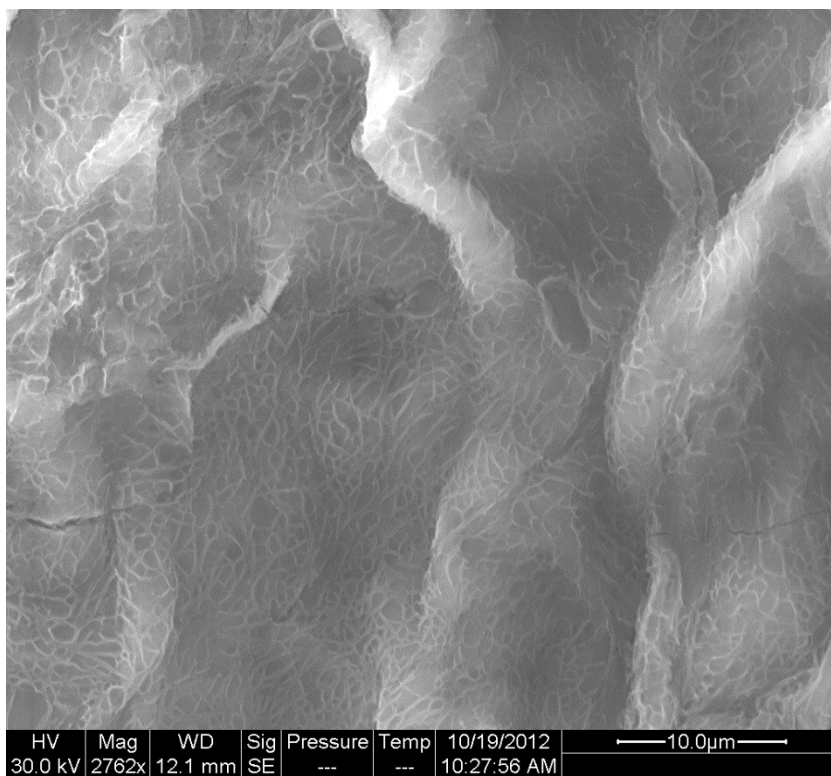
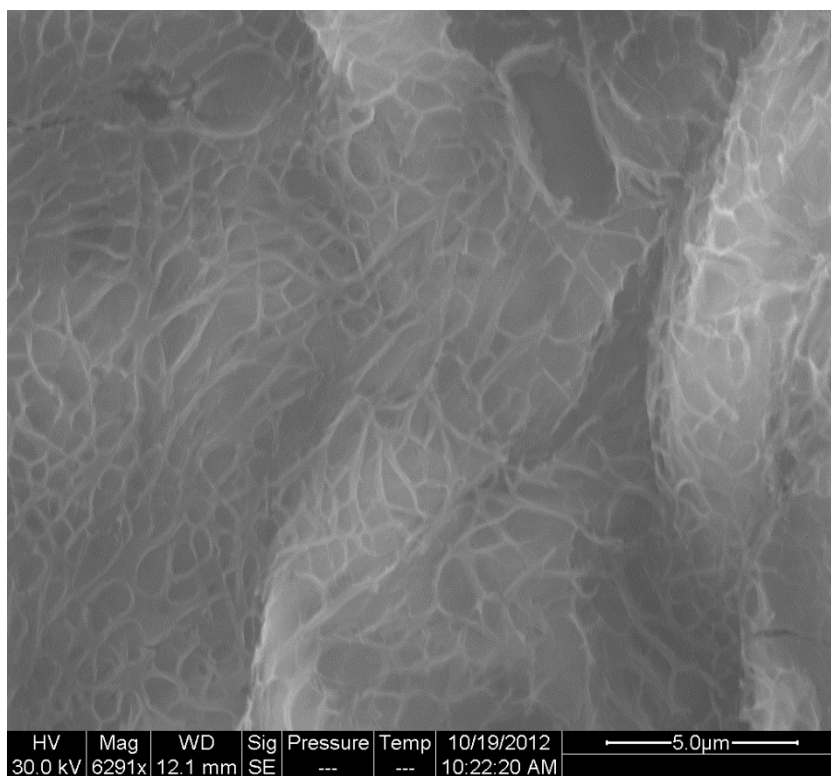


Figure S5. SEM Images of daisy chains from $1 \cdot 2PF_6$ in CH_2Cl_2

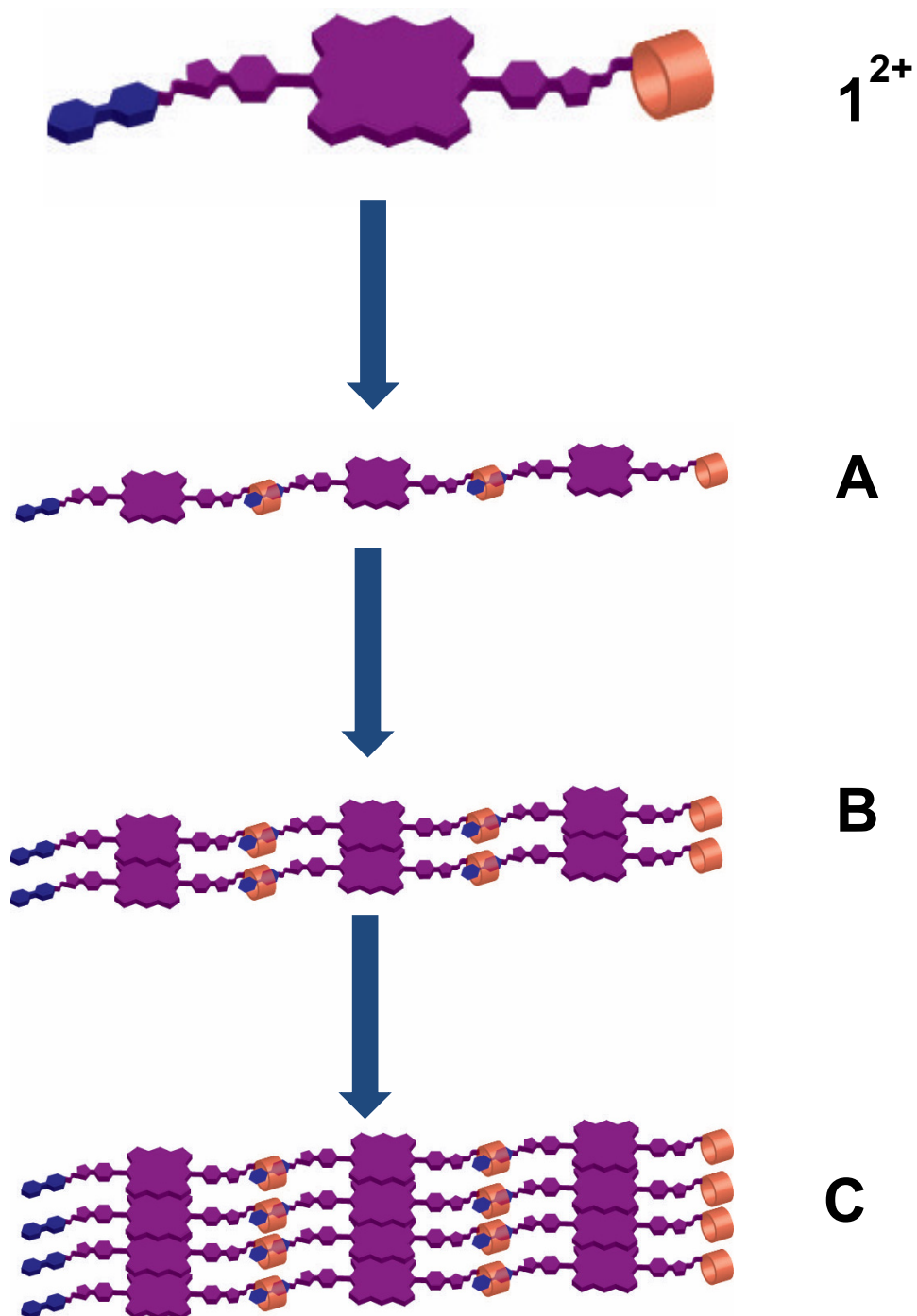


Figure S6. Graphical representation of the proposed mechanism for the gel formation from the daisy chains of 1^{2+} . At low concentration, the self-assembly of porphyrin 1^{2+} forms daisy chains (A). As the concentration is increased, these daisy chains further self-assemble to form discrete fibers (B) followed by the formation of large bundles (C) which eventually entangle with each other to form the gel material

S8. References.

- S1. F.S. Lu, S. Q. Xiao, Y. L. Li, H. B. Liu, H. M. Li, J. P. Zhuang, Y. Liu, N. Wang, X. R. He, X. F. Li, L. B. Gan, D. B. Zhu, *Macromolecules* **2004**, *37*, 7444.
- S2. N. L. Strutt, R. S. Forgan, J. M. Spruell, Y. Y. Botros, J. F. Stoddart, *J. Am. Chem. Soc.*, **2011**, *133*, 5668.
- S3. P. R. Ashton, R. Ballardini, V. Balzani, I. Baxter, A. Credi, M. C. T. Fyfe, M. T. Gandolfi, M. Gómez-López, M. V. Martínez-Díaz, A. Piersanti, N. Spencer, J. F. Stoddart, M. Venturi, A. J. P. White, D. J. Williams, *J. Am. Chem. Soc.* **1998**, *120*, 11932.